Proc. 11th New Zealand Geothermal Workshop 1989

TWO -PHASE FLOW STUDIES

J. Burnell, W. Kissling, M. McGuinness, A. McNabb, G. Weir, S. White, R. Young

Applied Mathematics Division
DSIR
Wellington New Zealand

Abstract

Numerical results from studies of two-phase 1D horizontal flow in finite blocks are examined. Timescales for pressure diffusion and saturation convection allow approximate analysis in some cases. Nonlinear effects are important, and lead to spreading travelling waves, single shocks and multiple shocks.

Introduction

Many geothermal reservoirs have both liquid and steam phases present in the natural state, or develop two-phase zones under production. The importance of the interaction between liquid and vapour phases is recognised in modelling geothermal reservoirs (White et al, 1971; Ingebritsen and Sorey, 1988; Pruess, 1985; Schubert and Straus, 1979).

Analytical work done to date on the governing equations for two-phase flow in a porous medium has traditionally involved taking linear approximations (Grant and Sorey, 1979; Grant, 1978; Garg, 1978; Moench and Atkinson, 1978), whereas these equations are nonlinear. Our overall aims have been to develop analytical or quasi-analytical solutions that include nonlinearity, as a check on the performance of geothermal simulators when simulating two-phase flow, and to improve our understanding of the possible responses of two-phase reservoirs to production and injection.

Our studies show that nonlinear effects, while challenging to cope with, are important, and produce some interesting results. Sorey et al (1980) also note the importance of nonlinear terms in their quasi-analytical study of two-phase flow to geothermal wells.

The cases looked at here reflect in their boundary conditions the importance of fracturing in geothermal reservoirs. We deal in particular with one-dimensional flow in a finite uniform porous medium, but the boundary conditions considered are realistic for a reservoir consisting of low permeability blocks separated by high permeability fractures, with this study then applying to one block in such a reservoir.

In this paper we will use three representative simulator results as case studies. In the first case a uniform pressure drop is imposed on the faces of a finite 1D block which has steady two-phase throughflow in the initial state. Saturation is also dropped at the block face, to a level such that a spreading drying front eventually enters the block. In the second case, a wetting front enters the block, as a shock. In the third case, throughflow speed is increased, and a wetting front enters the block, causing multiple shock formation.

The approach taken in this paper is to present some points of interest from the work done, leaving much of the mathematical detail to other publications (Burnell et al, 1988, 1989). This is work in progress.

The simulators used are MULKOM, courtesy of K. Pruess of Lawrence Berkeley Laboratory (Pruess, 1983), and a simulator written at AMD by S.P. White, as an extra check on results.

Governing Equations

We use the following porous medium equations, obtained by combining mass and energy conservation equations

$$\frac{\partial M}{\partial t} + \frac{\partial \Phi_M}{\partial x} = 0 = \frac{\partial E}{\partial t} + \frac{\partial \Phi_E}{\partial x} \qquad (1)$$

with Darcy's law. Here $M(P,S)$ and $E(P,S)$ are mass and energy densities with a functional dependence on pressure P and liquid saturation S. For a two-phase fluid in a porous medium they are given by

$$M \equiv \phi[S\rho_l + (1-S)\rho_v] \qquad (2)$$

$$E \equiv (1-\phi)\rho_m U_m + \phi[S\rho_l U_l + (1-S)\rho_v U_v] \qquad (3)$$

where ϕ is the porosity, ρ_l, ρ_v, ρ_m are the densities of the liquid and vapour phases and of the rock matrix, U_l, U_v, U_m are specific internal energies. The densities and specific internal energies are furictions of the pressure P, when two phases are present. The flux terms are (ignoring conduction and gravity)

$$\Phi_M = -F\frac{\partial P}{\partial x} \qquad (4)$$

$$\Phi_E = -hF\frac{\partial P}{\partial x} \qquad (5)$$

where

$$F = k\left(\frac{R_l}{\nu_l} + \frac{R_v}{\nu_v}\right), \qquad (6)$$

$$h = \left(\frac{h_l R_l}{\nu_l} + \frac{h_v R_v}{\nu_v}\right) \Big/ \left(\frac{R_l}{\nu_l} + \frac{R_v}{\nu_v}\right), \qquad (7)$$

where k is the absolute permeability, R_l and R, are the relative permeabilities of liquid and vapour phases, h_l and h_v are their specific enthalpies, and ν_l, ν_v are their kinematic viscosities.

A usefbl alternative form of these equations is obtained by eliminating second derivatives of pressure,

$$\frac{\partial E}{\partial t} - h\frac{\partial M}{\partial t} = F\frac{\partial h}{\partial x}\frac{\partial P}{\partial x}$$

or more explicitly

$$\mathcal{E}_P\frac{\partial P}{\partial t}+\mathcal{E}_S\frac{\partial S}{\partial t} = \left(F\frac{\partial h}{\partial P}\right)\left(\frac{\partial P}{\partial x}\right)^2 + \left(F\frac{\partial h}{\partial S}\right)\left(\frac{\partial P}{\partial x}\frac{\partial S}{\partial x}\right) \quad (8)$$

where

$$\mathcal{E}_P = \frac{BE}{ap} - \frac{\partial M}{\partial P}$$
$$\mathcal{E}_S = \frac{\partial E}{\partial S} - \frac{\partial M}{\partial S}.$$

Equation (8) is a hyperbolic equation for saturation which could be solved by the method of characteristics if pressure was known. The possibility of shock solutions is raised by this form.

The equation for pressure is obtained by eliminating the time derivative of saturation from equations (1),

$$J\frac{\partial P}{\partial t} = [-F\mathcal{E}_S]\frac{\partial^2 P}{\partial x^2} + \left[F\frac{\partial h}{\partial P}\frac{\partial M}{\partial S} - \mathcal{E}_S\frac{\partial F}{\partial P}\right]\left(\frac{\partial P}{\partial x}\right)^2 + \left[F\frac{\partial h}{\partial S}\frac{\partial M}{\partial S} - \mathcal{E}_S\frac{\partial F}{\partial S}\right]\left(\frac{\partial P}{\partial x}\frac{\partial S}{\partial x}\right) \quad (9)$$

where the Jacobian is

$$J = \frac{\partial M}{\partial S}\frac{\partial E}{\partial P} - \frac{\partial E}{\partial S}\frac{\partial M}{\partial P}. \quad (10)$$

The pressure equation can be interpreted as a diffusion equation for P. It is in general strongly coupled with the saturation equation (8).

Case A

The details of the numerical models set up as Cases A, B and C are summarised in Table 1. The Case A model is of a finite 1D block of uniform porous material with a steady two-phase flow through it initially, The pressure is then dropped at both ends, and liquid saturation is also reduced, to such a level that eventually a drier two-phase flow enters the block and sweeps through it. This might be representative of what happens in a fractured reservoir that initially has a two-phase natural throughflow, and is produced at time zero, rapidly dropping pressures and saturations in the highly permeable fracture system. This model then looks at the slower block response to this situation.

Plots of the pressure and liquid saturation changes in the block with time are in Figures 1 and 2. A discussion of pertinent features of these responses follows.

Early Time Response

This response is similar in all three cases, and is only mentioned here. For short enough times, the response is that of a semi-infinite block. Pressure and saturation changes in Figures 1 and 2 look proportional to each other.

This may be explained by ignoring the initial flow in comparison with the flow induced by the pressure drop at the boundaries at time zero. Then a similarity variable may be introduced (see also Sorey et al, 1980; O'Sullivan and Pruess, 1980; Burnell et al, 1988), for short enough times that the block is infinite-acting. Introducing

$$\eta = x/\sqrt{t} \quad (11)$$

into equation (8) leads to the exact equation

$$S' = -P'\left(\eta\mathcal{E}_P + 2F\frac{\partial h}{\partial P}P'\right) \Big/ \left(\eta\mathcal{E}_S + 2F\frac{\partial h}{\partial S}P'\right), \quad (12)$$

Table 1. Parameter values and initial and boundary conditions used in numerical models.

block length	2 m
rock density	2650 kg/m^3
rock specific heat	1000 J/kg °C
linear relative permeabilities	
residual saturations	0.3, 0.7

Initial Conditions, Case A and B

steady throughflow	
end pressures	37 b, 37.011 b
liquid saturation	0.685 at inflow
porosity	0.2
permeability	10^{-15} m^2

Boundary Conditions, Case A

drop pressure 3 b both ends
drop liquid saturation to 0.35 at inflow

Boundary Conditions, Case B

drop pressure 3 b both ends
drop liquid saturation to *0.65* at inflow

Initial Conditions, Case C

steady throughflow	
end pressures	35 b, 37 b
liquid saturation	*0.5* at inflow
porosity	0.005
permeability	10^{-16} m^2

Boundary Conditions, Case C

increase saturation to *0.65* at inflow

where the prime denotes differentiation with respect to the similarity variable η.

The existence of an approximate functional relationship between P and S may be checked by plotting P against S as in Figure 3, from early time numerical simulation results, Case A. There is clear numerical evidence in the heavy lines in Figure 3 of such a relationship. The kinks in the lines are due to the effect of discretisation on very early responses.

If pressure were known, equation (12) could be numerically directly integrated in η to give saturation exactly for the semi-infinite case. However, pressure is dependent on saturation through equation (9). In general the two equations must be solved together.

An approximate solution for pressure may be obtained by linearising equation (9) about some initial pressure P_0, to get

$$P'' + \frac{\eta}{2D}P' = 0, \quad (13)$$

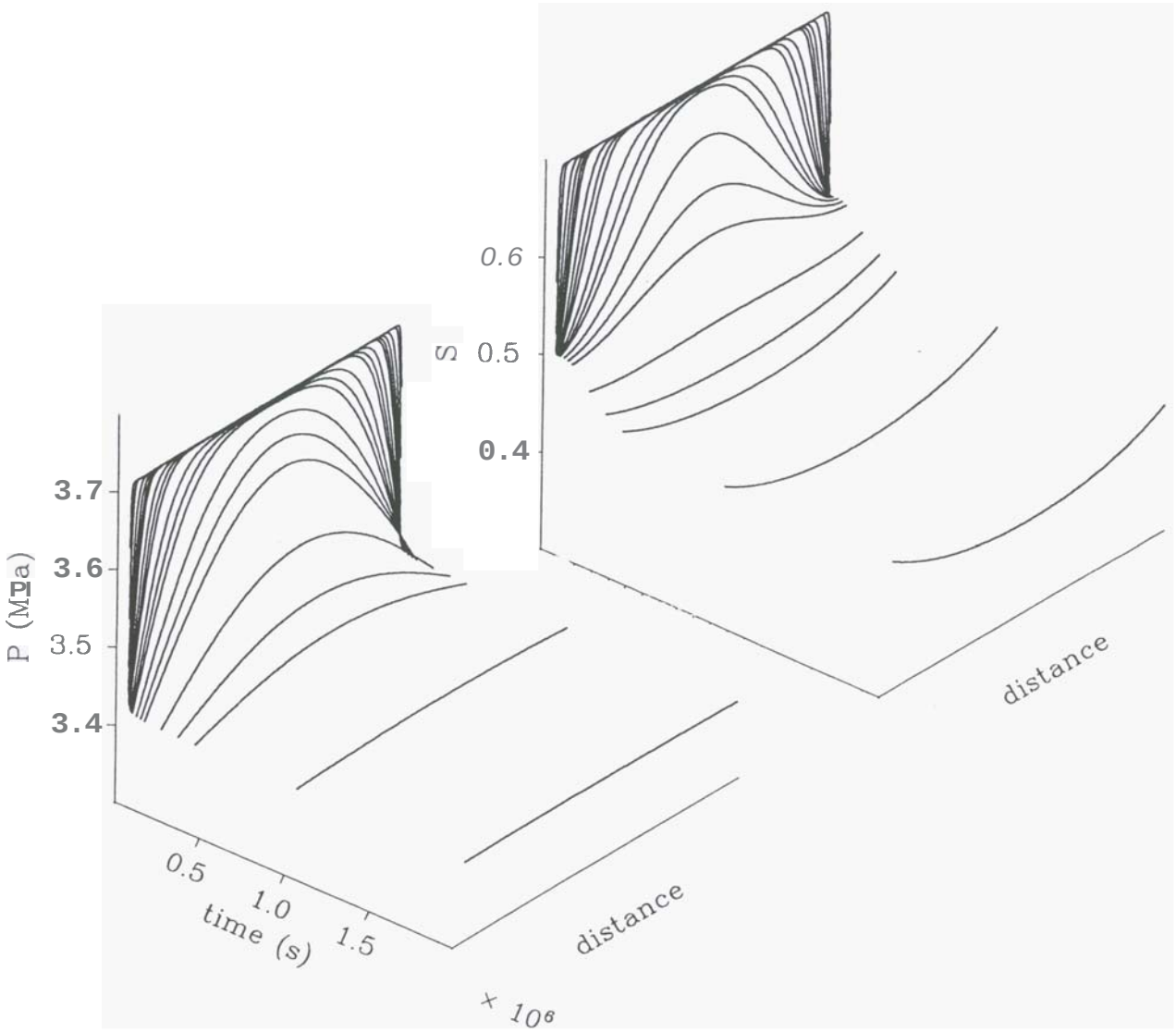
where

$$D \equiv -F\mathcal{E}_S/J. \quad (14)$$

D depends strongly on S. If this dependence is ignored, and D is assumed to be constant, remaining at its initial value, the solution of this equation is

$$P \sim P_0 - \Delta P\,\mathrm{erfc}\left(\frac{\eta}{2\sqrt{D}}\right),\ \Delta P \to 0, \quad (15)$$

where $\Delta P = P_0 - P_f$ is the (positive for production) pressure change imposed on the boundary at time zero.



Figures 1 and 2. Pressure and saturation responses for Case A at early times, plotted against time and position in perspective views. The early time response for Case B is similar.

Then taking the derivative of this solution gives

$$P' \sim -\Delta P \exp\left(\frac{\eta^2}{4D}\right)/\sqrt{\pi D},\ \Delta P \to 0. \qquad (16)$$

Using this approximate pressure solution in the exact relationship of equation (12) and numerically integrating the resulting ordinary differential equation in η gives a remarkably accurate value for S. The squares plotted in Figure 3 show the result of this process, with all coefficients assumed constant at their initial values.

Intermediate Time Responses

When the finite size of the block becomes important, saturation near the boundaries begins to change. Up until this time, saturation remains almost constant near the boundaries because of the existence of the similarity variable (equation (12)) and the constant pressure boundary condition. This response is similar in all three cases.

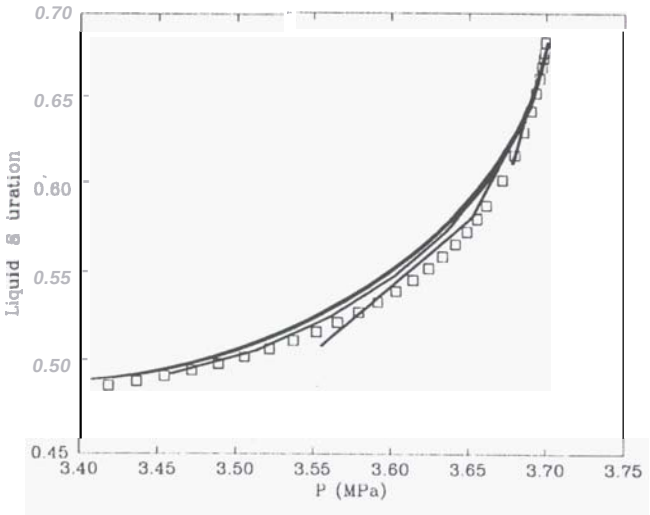


Figure 3. Pressure vs. saturation at early times, Case A.

The behaviour near the centre of the block is given by setting

$$\frac{\partial P}{\partial x} = \frac{\partial S}{\partial x} = 0$$

there by symmetry (ignoring any initial throughflow). Then equation (8) becomes

$$\mathcal{E}_P \frac{\partial P}{\partial t} + \mathcal{E}_S \frac{\partial S}{\partial t} = 0, \tag{17}$$

which may be numerically integrated to give the saturation drop at the centre of the block, given the pressure drop imposed on the boundaries. It is necessary to take account of the saturation dependence of the coefficients, while the pressure dependence may be ignored, so that

$$\int_{S_0}^{S_1} \frac{-\mathcal{E}_S}{\mathcal{E}_P}\, ds = -\Delta P. \tag{18}$$

The integration, which can be done explicitly in terms of log functions for linear relative permeabilities, gives accurate results for saturation at the centre of the block.

The cup shape seen in the saturation plots at intermediate times follows from noting that if $S = S(P)$, equation (8) can be integrated in time to give at the boundary

$$P - P_0 + \int_{S_0}^{S} \frac{\mathcal{E}_S}{\mathcal{E}_P}\, ds = \int_0^t \frac{F}{\mathcal{E}_P} \frac{\partial h}{\partial x} \frac{\partial P}{\partial x}\, dt \tag{19}$$

$$\sim \int_0^t \frac{F}{\mathcal{E}_P} \frac{\partial h}{\partial S} \frac{\partial S}{\partial P} \left(\frac{\partial P}{\partial x}\right)^2 dt \tag{20}$$

$$\equiv I. \tag{21}$$

The integral on the left-hand side is positive since $\frac{\partial S}{\partial P}$ and $\frac{\partial h}{\partial S}$ are both negative. This rearranges to give for large time

$$\int_{S_0}^{S_1} \frac{-\mathcal{E}_S}{\mathcal{E}_P}\, ds = -\Delta P + I. \tag{22}$$

That is, the integral I reduces the effective pressure drop, giving a smaller S drop at the boundaries than at the centre of the block (compare equation (18)). That is, a cup-shaped saturation curve is expected, as seen in Figure 2.

Late Time Response

This response is different in each of the three cases chosen. In case A a drier two-phase fluid enters at the left-hand side of the block when the direction of the pressure gradient there reverses. This saturation change moves through the block in a manner adequately approximated by the theory of expansion waves in hyperbolic systems. The two equations for saturation and pressure may be treated separately here because the time scales on which they operate are quite different. Three time scales are of interest:

1. A diffusive timescale for removal of pressure differences
2. A convective timescale for movement of saturation profiles
3. A timescale on which S responds to the flowing enthalpy profile

In this case A these three timescales are all different, with pressure diffusing away to a linear behaviour in times of the order of 10^6 seconds, and saturation changes convecting through the block in times of the order of 10^8 seconds. Saturation is almost constant along characteristics during this second behaviour, changing on the third timescale ($\sim 10^{10}$ seconds) due to the variation of flowing enthalpy with pressure.

With these comments in mind, equation (8) can be written

$$\frac{\partial S}{\partial t} + C \frac{\partial S}{\partial x} = -f, \tag{23}$$

where

$$C = \frac{F}{-\mathcal{E}_S} \frac{\partial h}{\partial S} \frac{\partial P}{\partial x},$$

and

$$f = \frac{F}{-\mathcal{E}_S} \frac{\partial h}{\partial P} \left(\frac{\partial P}{\partial x}\right)^2 - \frac{\mathcal{E}_P}{-\mathcal{E}_S} \frac{\partial P}{\partial t}.$$

C is a characteristic speed for saturation waves. The term $-\mathcal{E}_S$ is written this way because $\mathcal{E}_S$ is negative.

If it is assumed that $R_l + R_v = 1$, C reduces to

$$C = -\frac{k R_l'}{\phi(\mu_v R_l + \mu_l R_v)} \frac{\partial P}{\partial x}, \tag{24}$$

where μ is dynamic viscosity. Note that C depends on both S and P.

In case A, the fluid entering from the left-hand side is drier than the fluid downstream, so that no shock is formed. See Figure 4 for the saturation changes at later times. An expansion fan is inserted in the characteristic diagram. It enters at the left-hand side with zero velocity, and the saturation profile translates to the right and spreads out, as predicted by the dependence of the wave speed C on S (C increases when S is larger). The speed of translation of the profile is quite accurately approximated by assuming S is constant on the characteristics, that is, by ignoring the third timescale mentioned above, or by taking f in equation (23) to be zero.

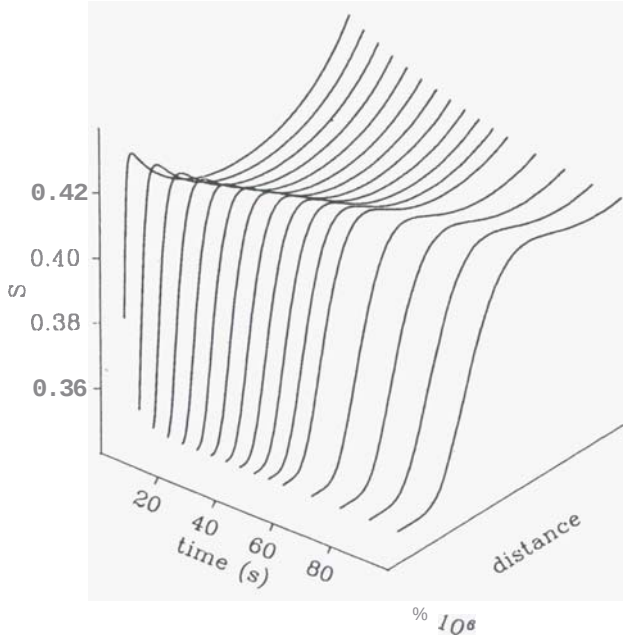


Figure 4. Late time liquid saturation response, Case A. An expansion wave enters from the left, or the end nearest the viewer.

Shocks

The possibility of shock formation is raised by the form of equation (23) together with the nonlinear speed C. A shock is a solution for S that has a discontinuous jump. Conservation of mass and energy across such a jump requires that

$$U \equiv \frac{\partial \mathcal{X}}{\partial t} = \frac{[\Phi_M]}{[M]} = \frac{[\Phi_E]}{[E]} \qquad (25)$$

where $\mathcal{X}(t)$ is the position of the shock front, and the square delimiters [] denote the difference across the shock.

Equation (25) implies that a saturation jump is accompanied by a jump in the pressure gradient (that is, a kink in the pressure profile). It also follows that volume flux Q is conserved across a shock, where

$$Q \equiv -\frac{k}{\mu_t}\frac{\partial P}{\partial x},$$

and

$$\frac{1}{\mu_t} \equiv \frac{R_l}{\mu_l} + \frac{R_v}{\mu_v}$$

defines a two-phase dynamic viscosity. It is possible to rewrite the entropy condition for shocks, using equation (25) to eliminate all pressure gradient terms, and assume that $R_l + R_v = 1$ for simplicity, to get

$$\alpha \left.\frac{\partial R_l}{\partial S}\right|_+ < \frac{R_{l-} - R_{l+}}{S_- - S_+} < \alpha^{-1} \left.\frac{\partial R_l}{\partial S}\right|_- , \qquad (26)$$

where $a \equiv \mu_{l+}/\mu_{l-}$, and subscripts + and − mean the variable is to be evaluated downstream and upstream of the shock respectively. For linear relative permeabilities, this simplifies to

$$S_+ < S_-, \qquad (27)$$

that is, for a shock to exist when both phases are mobile, the upstream (−) side must be *wetter* than the downstream (+) side.

A consequence of this is that production from a homogeneous two-phase reservoir with initial saturation increasing with distance away from the production well may result in shock formation. Shocks are also to be expected when injecting a fluid of higher saturation into a two-phase reservoir.

Case B

See Figure 5 for the numerical results of case B at later times. Only saturation responses are shown here — these are the most interesting. The early and intermediate time behaviours are the same as in case A. At late times a shock enters at the left-hand side of the block, because of the choice of saturation boundary condition there. The incoming fluid is wetter than the fluid in place, and the condition in equation (26) for the formation of a shock is satisfied. The shock travels at a speed given by equation (25).

Case C

The shock that enters in this case, illustrated in Figure 6, has a much higher velocity, so that the diffusive and convective timescales are no longer appreciably different. An intriguing phenomenon is seen in these plots, the apparent formation of multiple shocks in front of the primary shock. Standard analysis of the saturation equation in isolation from the pressure equation will not explain this behaviour.

It is necessary to restrict the time step size to 50 s to obtain the plot in Figure 6. This ensures the Courant condition is met. Larger time steps lead to a single shock that is not as steep.

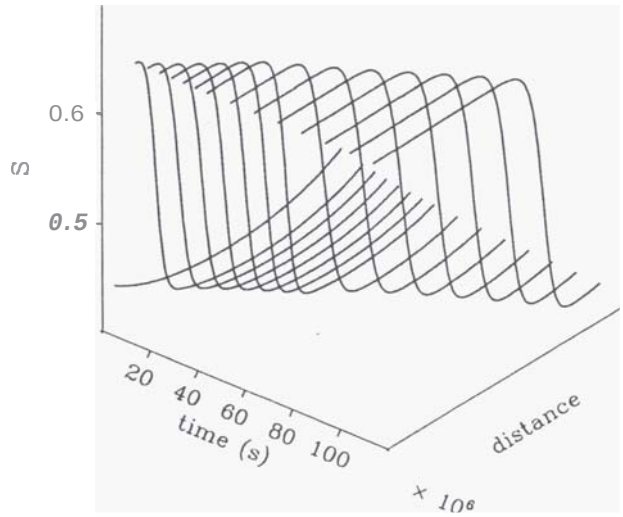


Figure 5. Late time liquid saturation response, Case B. A shock wave enters from the left, or the end nearest the viewer.

Conclusions

Nonlinear effects in two-phase flow with both phases mobile are important, leading in some cases to multiple shock formation. In other cases, the timescales on which pressure diffuses and saturation convects are different enough to allow approximate analysis.

References

Burnell, J., McNabb, A., Weir, G. and Young, R. (1988) Two-phase boundary layer formation in a semi-infinite porous slab, submitted to *Transport in Porous Media.*

Burnell, J., McNabb, A, Weir, G. and Young, R. (1989) The formation of boundary layers in two phase regions, *Proc. of Fourth Australasiun Conference on Heat and Mass Transfer,* held at Canterbury University, Christchurch, NZ, 9–12 May 1989, 543–550.

Burnell, J., McNabb, A., Weir, G., White, S. and Young, R. (1989) Response of porous medium to pressure changes: the example of a finite length, horizontal two-phase column, Proc. *of Fourth Australasian Conference on Heat and Mass Transfer,* held at Canterbury University, Christchurch, NZ, 9–12 May 1989, 721–727. Other papers are in preparation.

Garg, S.K. (1978) Preesure transient analysis for two-phaee (liquid .water/ steam) geothermal reservoirs, paper presented at 53rd Annual Fall Conference, SPE of AIME, Houston, Texas, Oct 143,1978.

Grant, M.A (1978) Two-phase linear geothermal pressure transients A comparison with single-phase transients, *N.Z.J. Sci.* 21355–364.

Grant, M.A. and Sorey, M.L. (1979) The compressibility and hydraulic diffusivity of a water-steam mixture, *Water Resour. Res.* 21648–686.

Ingebritsen, S.E. and Sorey, M.L. (1988) Vapor-dominated zones within hydrothermal convection systems: evolution and natural state, *J. Geophys. Res.,* 93 No. B11 13,635–13,655.

Moench, AF. and Atkinson, P.G. (1978) Transient pressure analysis in geothermal steam reservoirs with an immobile vaporising liquid phase, *Geothermics, 7* 253–264.

O'Sullivan, M.J. and Pruess, K. (1980) Analysis of injection testing of geothermal reservoirs, *Report LBL–10985,* Earth Sciences Division, Lawrence Berkeley Laboratory, Berkeley, California 94720.

Pruess, K. (1983) Development of the general purpose simulator MULKOM, *Annual Report 1982,* Earth Sciences Division Report LBL15500, Lawrence Berkeley Laboratory, Berkeley, California.

Pruess, K (1985) A quantitative model of vapor dominated geothermal reservoirs as heat pipes in fractured porous media, *Geoth. Resources Council Trans.* 9 Part II 353–361, August 1985.

Schubert, G. and Straus, J.M. (1979) Steam-water counterflow in porous media, *J. Geophys. Res.* 84 No. B4 1621–1628.

Sorey, M.L., Grant, M.A. and Bradford, E. (1980) Nonlinear effects in two-phase flow to wells in geothermal reservoirs, *Water Resour. Res. 16* (4) 767–777, August 1980.

White, D.E., Muffler, L.J.P. and Truesdell, A.H. (1971) Vapor-dominated hydrothermal systems compared with hot-water systems, *Econ. Geol. 66* 75–97.

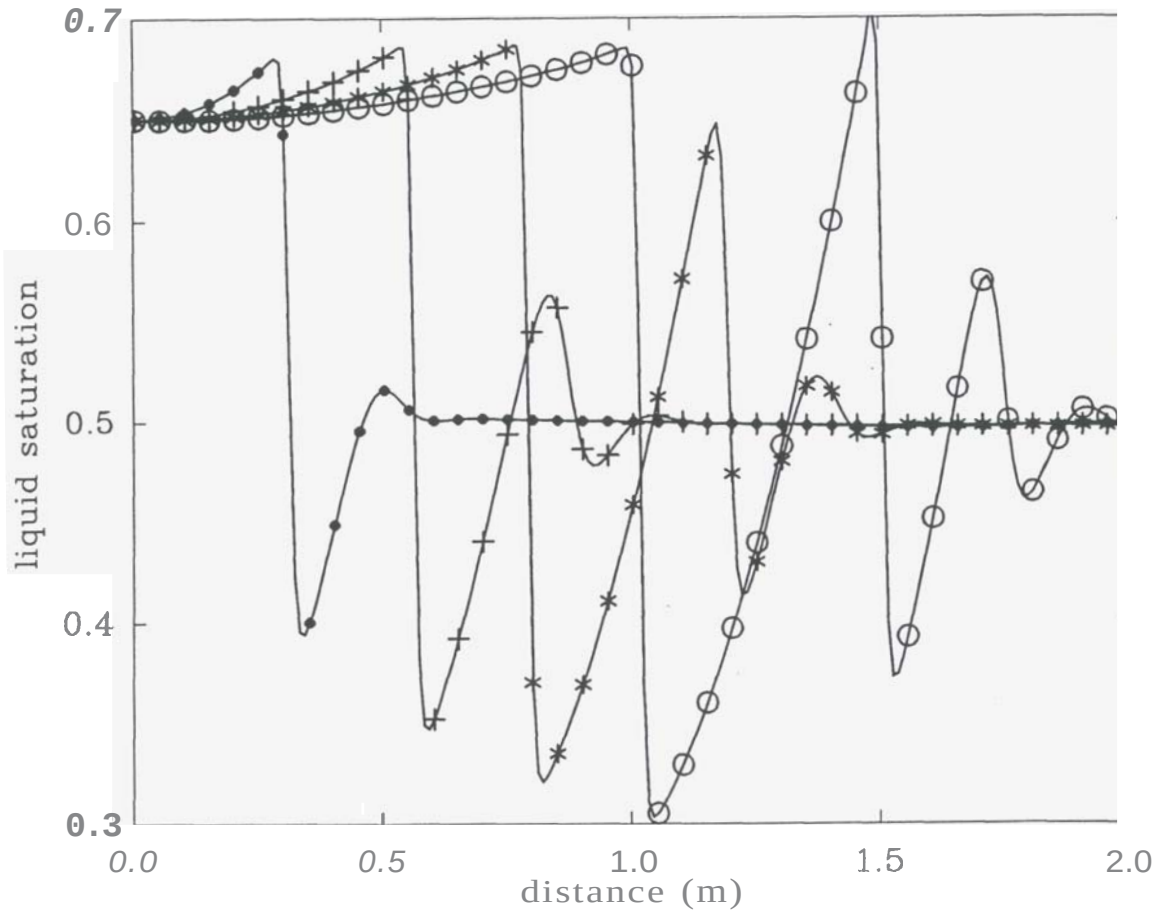


Figure 6. Late time liquid saturation response, Case C. A primary shock enters from the left, and appears to generate multiple secondary shocks in front. The times of the plots are 5×10^3, 10×10^3, 15×10^3 and 20×10^3 seconds.